JURNAL KARTIKA KIMIA

J. Kartika Kimia, May 2025, 8, (1), 142-149
Journal homepage: http://jkk.unjani.ac.id/index.php/jkk
P-ISSN: 2655-1322 E-ISSN: 2655-0938

Room Temperature Synthesis of Aluminium(III)-Benzenedicarboxylate Complex from Two Different Al(III) Salts

Nidatul Syarifah, Muhammad Farrel Yofandi, Qonitah Fardiyah, Yuniar Ponco Prananto*
Department of Chemistry, Faculty of Mathematics and Natural Sciences, Brawijaya University, Indonesia
*E-mail: prananto@ub.ac.id

DOI: https://doi.org/10.26874/jkk.v8i1.936

Received: 17 May 2025, *Revised*: 7 July 2025, *Accepted*: 10 July 2025, *Online*: 12 July 2025

Abstract

Al(III) complex with 1,4-benzenedicarboxylate ligand (Al-BDC) is a porous material that has the potential to be developed as an adsorbent or photocatalyst. This complex is often obtained by the solvothermal method at high temperature. This paper reports the synthesis of Al-BDC complex by solution method at room temperature from two different types of Al(III) salts, namely nitrate salt (complex 1) and chloride salt (complex 2). The synthesis of Al-BDC was conducted with Al(III):H_2-BDC mol ratio of 2:3. The synthesized complexes were characterized by ATR-IR, powder XRD, UV Vis–DRS, and DTA–TGA. The results showed that white powders were obtained with a yield of 75.8% (complex 1) and 65.7% (complex 2). The presence of BDC ligands in both complexes was confirmed by the presence of typical absorption bands of C=O, C-O, and Al-O functional groups in their infrared spectra. Both complexes have different surface morphology and average crystallite sizes (28.63 nm – complex 1; 34.98 nm – complex 2), but the powder X-ray diffraction patterns, DTA-TGA thermograms, UV Vis-DRS spectra, and band gap energy values of both complexes are considerably identical. Powder XRD diffraction analysis of both complexes shows a pattern that is identical to the known compound with a formula of $\{[Al(OH)(BDC)]\cdot(H_2BDC)_{0.69}\}_n$ (CCDC No. 2179625) in which the compound forms 3D polymeric structure with terephthalic acid occupies the voids.

Keywords: Aluminium(III), green synthesis, metal-organic frameworks, porous material, terephthalate

1 Introduction

Metal-Organic Frameworks (MOFs) are a porous polymer formed by a self-assembly process between inorganic metal ions or groups and organic ligands as a bridge to form a porous 3-dimensional material [1]. MOF has an important role in various applications due to its regular pore structure, large pore size, and high surface area [2]. MOF provides various active functional sites that have good chemical resistance, thermal stability and chemical functionality that can be designed for various applications [3]. MOF is often applied for catalysis, optics, gas storage, bioimaging, drug delivery, conductivity, and adsorbents of inorganic or organic pollutants in wastewater [4].

In recent years, Al-MOFs have attracted significant attention as promising candidates for functional materials. Various types of Al-MOFs have been successfully synthesized, such as Al-tartrate [5], Al-fumarate [6], Al-succinate [7], Al-BTC [8], and Al-BDC [9], each exhibiting different characteristics and structures depending on the type of ligand used. In this study, the material of focus is Al-BDC, one of which is known as MIL-53(Al).

MIL-53(Al) is included as Aluminum-based MOF that is widely developed. Aluminum ion (Al^{3+}) is used as the metal center and 1,4-benzenedicarboxylic acid (BDC) is used as ligand precursor. Aluminum is one of the most abundant metals in nature (8.2 wt% in the earth's crust) and has an affordable price [10]. Meanwhile, BDC is commercially available with two carboxylate groups in the *para* position and benzyl ring in the middle (**Fig. 1**), making the ions easy to coordinate with metal ions in several coordination modes (terminal, bridge, and chelate) [11]. The BDC ligands are rigid and sturdy, thus it forms Al-MOF materials with high structural stability when reacts with Al^{3+}.

Al-BDC has interesting properties, a non-toxic materials with high porosity and large surface areas [9]. Therefore, Al-MOF is often applied as gas adsorption [12], sensor [4], heterogeneous catalyst [13], drug delivery [14], etc. Al-BDC also has the potential as an adsorbent for metal ions [15], for gas [9], or organic waste

[16]. Al-BDC also gain interest over other MOFs, related to its breathing effect and resistance to hydrolysis [9], thus that it can be applied for wastewater treatment. Zokaee *et al* [17] reported that Al-BDC has a band gap of 3.54 eV and was applied for methylene blue dye photocatalysis.

Al-BDC complex has been synthesized using several method, namely solvothermal [18], hydrothermal [9], microwave [19], ultrasound [20], grinding (solvent free) [21], and reflux [22] methods. Al-BDC that was previously synthesized by hydrothermal method form octahedral $AlO_4(OH)_2$ chains that share corners, connected by carboxylate groups from the BDC ligands and then forming a three-dimensional structure with diamond-shaped pores [9].

Al-BDC is commonly synthesized using solvothermal method, which requires long reaction time and high temperature, in some cases using organic solvent. This condition is unfavourable for large scale production due to high energy consumption and delicate process. Exploration of greener synthetic method to reduce the reaction time is being carried out and other alternative methods have been developed [23]. In this study, a solution method using direct mixing method was proposed. The synthesis was carried out at room temperature in a one-stage reaction; thus, it is simpler, more efficient, does not require higher energy, and use water as solvent. Variations of Al^{3+} metal salts were also studied, to study the role of anion towards the characteristic of the Al-BDC.

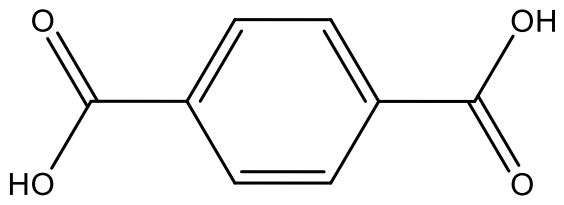

Figure 1 Structure of 1,4-benzenedicarboxylic acid (H_2-BDC), also known as terephthalic acid

2 Method

2.1 Materials and Instrumentation

The materials used in this research were $Al(NO_3)_3.9H_2O$, $AlCl_3.6H_2O$, terephthalic acid (HOOC-C_6H_4-COOH), NaOH, and water.

Instrumentation for analysis purposes used were ATR-IR (Shimadzu IRSpirit–T), powder-XRD (PANalytical XPert3 Powder), UV-Vis DRS (Specord 200 Plus), DTG (Shimadzu (Simultaneous DTA-DTG-60), SEM (Hitachi TM 3000).

2.2 Synthesis of Al-BDC Complexes

The synthesis of Al-BDC was carried out by solution method, by mixing Al(III) and H_2-BDC solutions in an open vial with Al(III):H_2-BDC mol ratio of 2:3. Two metal solutions were prepared by separately dissolving $Al(NO_3)_3{\cdot}9H_2O$ (750 mg; 2 mmol) and $AlCl_3{\cdot}6H_2O$ (483 mg; 2 mmol) with 20 mL of water each. The ligand solution was prepared by dissolving the H_2-BDC (498 mg; 3 mmol) with 40 mL of 6M NaOH solution. After the metal and ligand solutions were mixed, the solution pH was then adjusted at 7 and kept stirred with a magnetic stirrer for 1 hour. Next, the solution was filtered off using Whatman paper No. 41 and the solid was washed using warm water. The solid product was then dried in an oven at 110 ºC for 3 hours and stored in a desiccator for 3 days. The dry solid was then weighed to determine the yield. Product obtained from the nitrate salt is coded as complex 1, whereas product obtained from the chloride salt is coded as complex 2.

2.3 Characterization of Al-BDC Complexes

Complex 1 and complex 2 were all characterized by infrared spectroscopy (ATR-IR), powder X-ray diffraction (PXRD), thermal gravimetry (DTA-TGA), scanning electron microscopy (SEM), and UV Vis – DRS spectrophotometry.

The ATR-IR analysis was performed 4000-400 cm^{-1} to determine the typical functional groups of the BDC ligand that present in the complex. The PXRD analysis was conducted at 2θ angles of 10º to 60º using Cu-Kα radiation (λ = 1.541874 Å) to determine the average crystallite size by the Debye-Scherrer approach (**Eq. 1**), and to assign the structure of the complex:

$$D = \frac{k \times \lambda}{\beta \times cos\ \theta} \qquad \text{(Equation 1)}$$

Note: D is crystal size (nm), k is the shape factor (0.9), λ is the wavelength of the X-ray, 0.1542 nm, and β is the full width at half (FWHM) of the peak at 2θ in the pattern, and θ is the angel measured.

Furthermore, identification of the compound was carried out through pattern matching between the experimental powder diffraction data and reference patterns from the Cambridge Crystallographic Data Center (CCDC), assisted by HighScore software. The DTA-TGA analyses

were carried out at 30 – 600 °C with an increasing rate of 10 °C/minute to determine the thermal stability and decomposition profile of the complex. The SEM was performed at magnifications of 1,000 and 5,000. The UV-Vis DRS analysis was done by measuring the absorbance at 200–800 nm to determine the maximum absorption and band gap energy level of the complex by the Tauc plot method.

3 Result and Discussion

3.1 Synthesis of Al-BDC Complexes

Al-BDC complexes were synthesized at room temperature in one pot reaction by mixing and stirring both aqueous solutions of metal and ligand until precipitate product were obtained. This one step reaction is very simple, and yet effective, and used environmentally friendly solvent and mild condition. To differentiate the complex, the precipitated products were coded as complex 1 (from the nitrate salt) and complex 2 (from the chloride salt). Both the nitrate and chloride salts resulted in white solids (**Fig. 2**).

(a) (b)

Figure 2 White powder of complex 1 (a) and complex 2 (b)

3.2 Result of Al-BDC Characterization.

Infrared spectra of complex 1 and complex 2 show identical results (**Fig. 3**). Infrared spectra give a sharp absorption at 1697 cm^{-1}, which correspond to carbonyl group (C=O), sharp peaks at 1608 and 1414 cm^{-1}, which related to the asymmetric and symmetric stretching vibrations of the carboxylate (-COO) group from the BDC. There is also absorption at 1507 and 1437 cm^{-1}, which is assigned to the C=C vibration of the benzene ring [24]. Absorption at 981 cm^{-1} is related to the bending vibration of the hydroxyl group in octahedral $AlO_4(OH)_2$ with *trans* corner-sharing [20]. A sharp absorption at 750 cm^{-1} corresponds to the bending vibration of C–H of the benzene ring [24], whereas a sharp absorption at 594 cm^{-1} relates to the stretching vibration of the Al-O bond, indicating the coordination between Al^{3+} and BDC ligand [25].

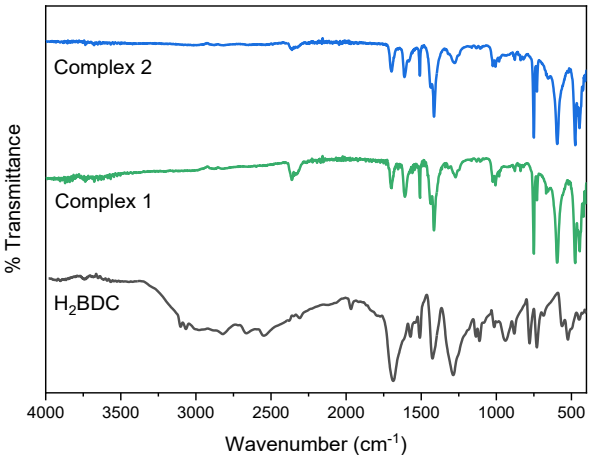

Figure 3 Infrared spectra of complex 1, complex 2, and the ligand precursor of H_2-BDC

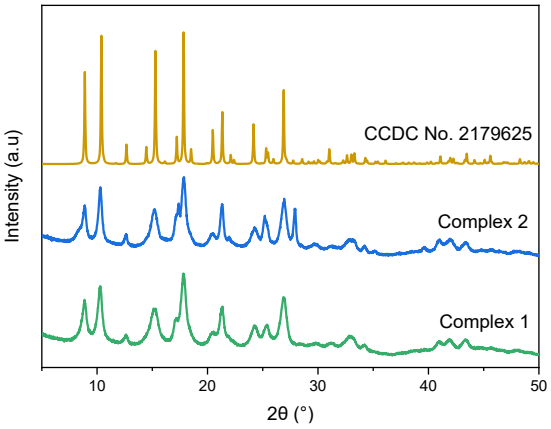

Figure 4 Diffraction patterns of complex 1, complex 2, and Al-BDC compound from CCDC No. 2179625

Analysis using Powder-XRD was observed in 2θ angle of 5º to 50º. The diffractogram patterns of complex 1 and complex 2 are shown in the **Fig. 4**. Based on the results of the XRD characterization, the diffractogram patterns of both products show the same pattern. Both products have main peaks at 2θ of 8.9°, 10.3°, 12.6°, 15.26°, 17.8°, 26.91°. These results are the same as those reported by [26]–[28], in which the MIL-53(Al) was synthesized by hydrothermal method [27] and showed peaks at 2θ of 8.9°, 10.4°, 12.7°, 15.4°, and 17.8°. The average crystal sizes of complex 1 and complex 2 are 28.63 nm and 34.98 nm, respectively, based on the Debye Scherrer equation, calculated using the XRD Crystallite (grain) Size Calculator. Moreover, wide base of the diffraction peak observed in both complexes indicate the low crystallinity of the product, which also means that there is an amorphous product present in the sample. The crystallinity degree of both complexes is about 35.7% and 37.0% for complex 1 and complex 2,

respectively. The low crystallinity degree is frequently observed in direct mixing method, which is unsuitable for optimal crystal growth of crystal due to high rate of nuclei formation.

These results (**Fig. 4**) are also checked with previously reported Al-BDC in the Cambridge Crystallographic Data Center (CCDC), in which Al-BDC reported in this study is identical to compound No. 2179625 [26], [29]. The diffractogram peaks of complex 1 and complex 2 show that the synthesized complexes have a good agreement with the reference MIL-53(Al) or $\{[Al(OH)(BDC)]\cdot(H_2BDC)_{0.69}\}_n$. The simple synthesis procedure used in this work produces the same Al-BDC complex that has polymeric networks, as shown in **Fig. 5**. Based on the database, this MIl-53(Al) complex compound has an *orthorhombic* crystal system with a space group $P2_1/n$ (a = 105.224(4) Å, b = 12.2441(5) Å, c = 17.0143(6) Å, β = 89.99(1)°). In the crystal structure of MIL-53(Al), the terephthalic acid molecule occupies the pores and remains in its molecular form [30].

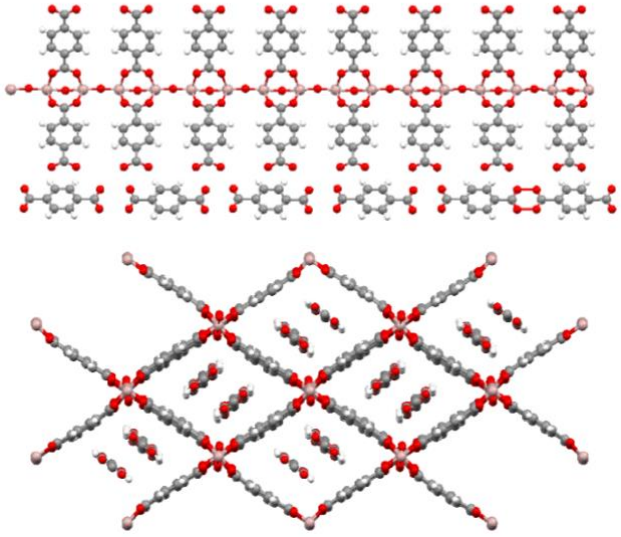

Figure 5 Crystal packing of $\{[Al(OH)(BDC)]\cdot(H_2BDC)_{0.69}\}_n$ viewed from two different angles

The DTA-TGA analysis was conducted from 30 to 600 ºC, and the thermograms of both complexes are shown in **Fig. 6**. TGA results show that complex 1 and complex 2 have nearly identical thermal stability, in which both have decomposition patterns in almost the same temperature range. This shows that differences in Al(III) salt sources did not affect the thermal stability of the synthesized complex. Both complexes show decomposition profile in three stages. In the first stage, complex 1 experienced a gradual decrease in mass in the temperature range of 30 to 280 °C by 12%. In the second stage, a sharp decrease began at 320 - 390 °C by 15%, and followed by the third stage, a significant sharp decrease by 46% occurred at 500-600 °C. Meanwhile, complex 2 undergo mass loss in the temperature range around 30 to 280 °C by 14%, 330 to 390 °C by 18%, and finally 480 to 580 °C by 47%.

The mass loss in both complexes in the first stage is most likely caused by the release of free water molecules and coordinated water in the crystal structure. In the second stage, partial decomposition of the organic ligand of BDC may be occurs. Meanwhile, the sharp decrease in the third stage indicates the decomposition of the Al-BDC polymeric framework, leaving inorganic residues, such as Al_2O_3 [3]. After heating around 600 °C, complex 1 decomposes and leaving around 20% of residual sample, whereas complex 2 leaving around 12% of residual sample. Based on this formula, $\{[Al(OH)(BDC)]\cdot(H_2BDC)_{0.69}\}_n$, decomposition into Al_2O_3 resulting in around 16% residue. This difference is probably due to different level of dryness of the sample, or incomplete organic decomposition. In addition, the DTA profile of both complexes show very similar patterns, only the decomposition temperature is slightly shifted, but the sequence and process are identical.

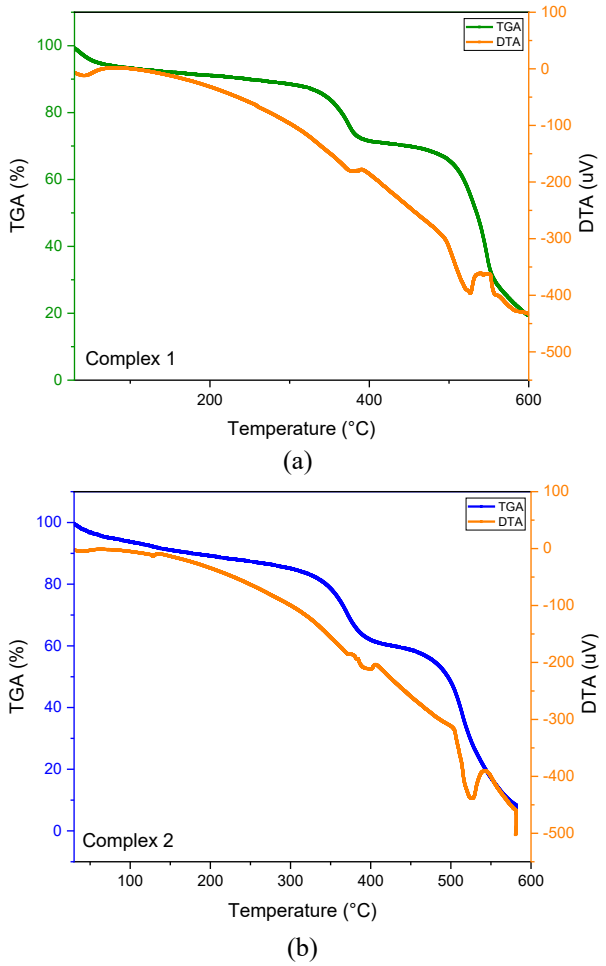

Figure 5 DTA-TGA thermogram of (a) complex 1 and (b) complex 2

The optical properties of the synthesized Al-BDC were investigated through UV–vis DRS analysis. Complex 1 absorbs at a maximum wavelength of 293 nm while complex 2 absorbs at 295 nm, as shown in **Fig. 7**. This can be due to the π–π* electronic transition of the aromatic ligand BDC system and the contribution of ligand to metal charge transfer (LMCT). Furthermore, the band gap energy of both materials was analyzed using Tauc plot. In the Tauc plot, the band gap energy (Eg) value of Al-BDC is determined from the relationship graph between $(\alpha h\upsilon)^2$ and $h\upsilon$ [31]. The band gap energy results for complex 1 are 3.76 eV while for complex 2 is 3.73 eV. The results of the Al-BDC band gap energy are slightly different from those reported by others [31], which is 3.65 eV. Nevertheless, this energy level also indicate that the complex may be utilized as a photocatalyst.

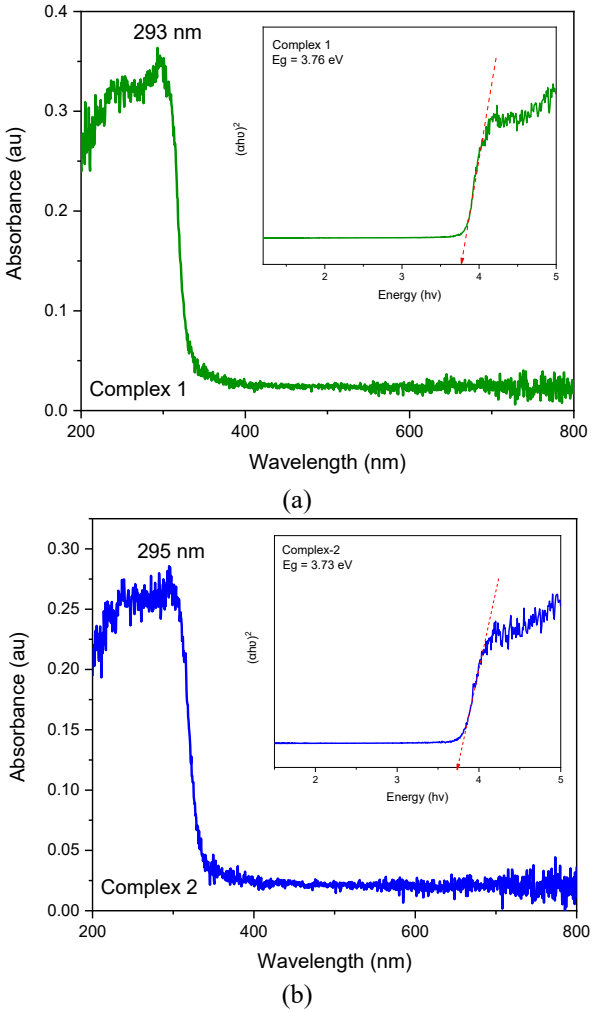

Figure 7 Maximum absorption and band gap energy of complex 1 (top) and complex 2 (bottom)

SEM analysis was observed at 1,000x and the images are shown in **Fig. 8**. The SEM image reveal that complex 1 has irregular shape and forms aggregates, while complex 2 forms a plate-like structure that is stacked each other. This suggest that the anion of the Al salt may influence the morphology of the synthesized complex. Chloride ions are known to be more effective in directing crystal growth compared to nitrate ions. This is in accordance with the crystallite data from the XRD analysis, in which complex 2 has a larger crystal size than that of complex 1, indicating better crystallization. This is also supported by the particle size distribution data (**Fig. 8**), which shows that better crystallization led to the formation of bigger crystallite size. This anion effect on particle morphology is also observed in other aluminium-MOF [6, 32], with fumarate ligand.

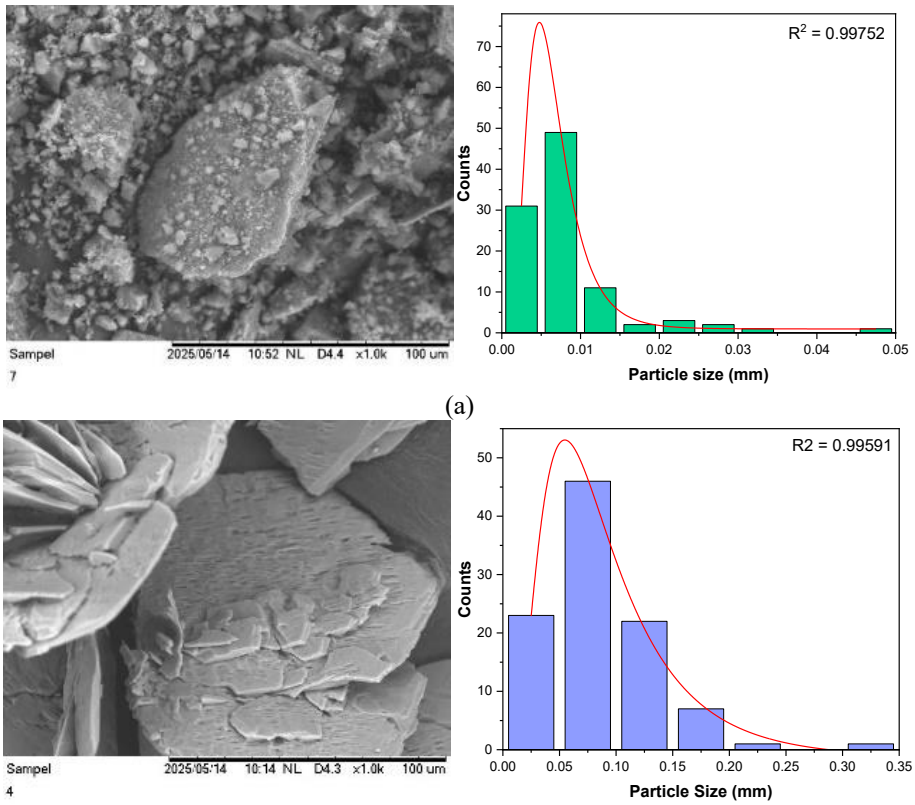

Figure 6 Surface morphology (magnification of 1,000x) and particle size distribution of complex 1 (a) and complex 2 (b)

This study finds that the band gap energy level of the Al-BDC obtained from room temperature reaction using water as solvent, correlates with the crystal morphology and crystallinity degree; the better the crystallinity, the lower the band observed. Moreover, the smaller the crystallite size, the smaller band gap energy obtained. This study also opens a possible greener pathway for the synthesis of Al-BDC complex. Compared to the solvothermal method, particularly that use dimethylformamide as solvent, the use of water as solvent resulting in Al-BDC complex with slightly different properties but the Al-BDC remains possible to be used for photocatalyst.

4 Conclusion

White crystalline solid of Al-BDC complexes were synthesized using a direct mixing method at room temperature using two different Al(III) salts, namely nitrate and chloride. The type of aluminum salt used in the synthesis affects the yield and the characteristic of the synthesized Al-BDC. Although both Al-BDC complexes have different surface morphology and average crystallite sizes (28.63 nm – complex 1 and 34.98 – complex 2), powder X-ray diffraction patterns, DTA-TGA thermograms, UV Vis-DRS spectra, and band gap energy values of both complexes are considerably identical. Powder XRD diffraction analysis of both complexes also confirms that the Al-BDC synthesized in this work is identical to a known compound of $\{[Al(OH)(BDC)]\cdot(H_2BDC)_{0.69}\}_n$, in which the complex forms 3D polymeric structure.

Acknowledgement

All authors acknowledge the Department of Chemistry (FMIPA) and Integrated Research Laboratory (LRT) of Universitas Brawijaya, Indonesia for any support given, including the XRD facility (PANalytical X'Pert3 Powder). Part of this research was also supported by the PPS-PTM Research Grant 2024 (Contract No. 00309.116/UN10.A0501/B/PT.01.03.2/2024) from the Indonesian Ministry of Higher Education, Science and Technology.

References

[1] Uthappa UT., Ajeya KV., Sannasi V., Lee SG., Sohn EH., Chang BJ., Park IJ., Kim JH., Kurkuri MD., & Jung HY., 2024, Green aluminum metal-organic frameworks (Al-

MOFs) supported on commercial activated carbon for enhanced removal performances of industrial fluoride pollutants, *Journal of Water Process Engineering*, 63, 1-10. https://doi.org/10.1016/j.jwpe.2024.105450

[2] Abdelhameed RM., Taha M., Abdel-gawad H., & Hegazi B., 2021, Amino-functionalized Al-MIL-53 for dimethoate pesticide removal from wastewater and their intermolecular interactions, *Journal of Molecular Liquids*, 327, 1–9. https://doi.org/10.1016/j.molliq.2020.114852

[3] Bansal P., Mishra D., Vijayakumar A., & Chatterjee S., 2023, Aluminium terephthalate (Al-BDC) based metal organic framework decorated carboxymethylated filter cloth for defluoridation application, *Journal of Environmental Chemical Engineering,* 11(3), 1-14. https://doi.org/10.1016/j.jece.2023.110233

[4] Alaysuy O., Alorabi AQ., Aljohani MM., Alluhaybi AA., Snari M., Bedowr NS., Shah R., & El-metwaly NM., 2024, Aluminum MOF-based sensor for simultaneous colorimetric and fluorometric detection of Co^{+2} in electroplating wastewater samples and recovery of Pd^{+2} ions from electronic wastes, *Journal of Water Process Engineering,* 59, 1-12. https://doi.org/10.1016/j.jwpe.2024.104993

[5] Prananto YP., Purwonugroho D., Dzakwan MNT., Setianingsih T., & Syarifah N., 2025, Synthesis of microcrystalline aluminium(III)-tartrate by hydrothermal reaction: Effect of tartrate precursor and mol ratio, *Acta Chimica Asiana*, 8(1), 599–605. https://doi.org/10.29303/aca.v8i1.244

[6] Moumen EB., Bazzi L., Hankari SE., 2022, Aluminum-fumarate based MOF: A promising environmentally friendly adsorbent for the removal of phosphate, *Process Safety and Environmental Protection*, 160, 502–512. https://doi.org/10.1016/j.psep.2022.02.034

[7] El Salam HMA., 2023, Bio-Sustainable Alternatives Synthesis of Nanoporous Activated Carbon @Al-MOF for the Adsorption of Hazardous Organic Dyes from Wastewater, *Water, Air, and Soil Pollution*, 234(9), 1–14. https://doi.org/10.1007/s11270-023-06572-6

[8] Zhuang S., Huang H., Xiao Y., Zhang Z., Tang J., Gates BC., & Yang D., 2021, Pair sites on Al_3O nodes of the metal-organic framework MIL-100: Cooperative roles of defect and structural vacancy sites in methanol dehydration catalysis, *Journal of Catalysis*, 404, 128–138. https://doi.org/10.1016/j.jcat.2021.09.006

[9] Lopes J., Miranda D., Pereira T., Abreu D., Souza DDP., Coelho I., Stavale F., Sant S. De, Oliveira A., Cristina L., & Moura D., 2023, case study for an eco-design of aluminum terephthalate metal-organic framework-MIL-53 (Al) for CO_2 and methane adsorption, *Sustainable Materials and Technologies*, 37, 1-15. https://doi.org/10.1016/j.susmat.2023.e00689

[10] Al M.-, Venturi DM., Guiotto V., Amato RD., Calucci L., Signorile M., Taddei M., Crocellà V., & Costantino F., 2023, Solvent-free synthesis of a new perfluorinated MIL-53 (Al) with a temperature-induced breathing effect, *Molecular Systems Design & Engineering*. 8(5), 586–590. https://doi.org/10.1039/d2me00280a

[11] Finisia Y., Tjahjanto RT., & Prananto YP., 2024, Effect of solvent in the solvothermal synthesis of nickel (II) -terephthalate complex, *Acta Chimica Asiana*, 7(2), 487–493. https://doi.org/10.29303/aca.v7i2.198

[12] Yu Y., Shang M., Kong L., Li X., Wang L., & Sun T., 2023, Influence of ligands within Al-based metal-organic frameworks for selective separation of methane from unconventional natural gas, *Chemospher,* 321, 1-11. https://doi.org/10.1016/j.chemosphere.2023.138160

[13] Khani Y., Kumar A., Sung B., Hyun C., Ali M., Jeon B., & Park Y., 2024, Al-MIL-53 metal-organic framework supported Ru catalyst for selective hydrodeoxygenation of lignin-derived phenols into cyclohexane, *Chemical Engineering Journal*, 490, 1-15. https://doi.org/10.1016/j.cej.2024.151637

[14] Stillman ZS., Decker GE., Dworzak MR., Bloch ED., & Fromen CA., 2023, Aluminum -based metal – organic framework nanoparticles as pulmonary vaccine adjuvants, *Journal of Nanobiotechnology*, 21(1), 1–20. https://doi.org/10.1186/s12951-023-01782-w

[15] Alatawi ISS., Ibarhiam SF., Alrashdi KS., Alkhamis KM., Alaysuy O., Alkhathami ND., Alamoudi WM., & El-metwaly NM., 2024, Removal of metal ions by adsorption on Al based metal organic frameworks, *Inorganic Chemistry Communications*, 165, 0–8. https://doi.org/10.1016/j.inoche.2024.112514

[16] Qi L., Jiang H., Lin T., Chang X., & Jiang B., 2021, Fabrication of MIL-53 (Al) based composites from biomass activated carbon (AC) for ef fi cient p-nitrophenol adsorption from aqueous solution, *Journal of the Taiwan Institute of Chemical Engineers,* 127, 220–227. https://doi.org/10.1016/j.jtice.2021.08.020

[17] Zokaee Z., Mohammad N., & Reza M., 2022, Synthesis of visible light activated metal-organic framework coated on titania nanocomposite (MIL-53 (Al)@ TiO 2) and dye photodegradation, *Journal of Solid State Chemistry*, 307, 1-10. https://doi.org/10.1016/j.jssc.2021.122747

[18] Salionov D., Semivrazhskaya OO., Casati NPM., Ranocchiari M., Bjelić S., Verel R., van Bokhoven JA., & Sushkevich VL., 2022, Unraveling the molecular mechanism of MIL-53(Al) crystallization, *Nature Communications*, 13(1), 1–9. https://doi.org/10.1038/s41467-022-31294-4

[19] Sun L., Yin M., Li Z., & Tang S., 2022, Facile microwave-assisted solvothermal synthesis of rod-like aluminum terephthalate [MIL-53(Al)] for CO_2 adsorption, *Journal of Industrial and Engineering Chemistry* 112, 279–286. https://doi.org/10.1016/j.jiec.2022.05.021

[20] Ahadi N., Askari S., Fouladitajar A., & Akbari I., 2022, Facile synthesis of hierarchically structured MIL - 53 (Al) with superior properties using an environmentally - friendly ultrasonic method for separating lead ions from aqueous solutions, *Scientific Reports*, 53, 1–17. https://doi.org/10.1038/s41598-022-06518-8

[21] Chong KC., Lai SO., Chong WC., Thiam HS., Yong CH., Kam HK., Long S., Long JS., Tunku U., Rahman A., & Long JS., 2024, Performance Determination of Aluminium Metal Organic Framework in Carbon Dioxide Gas Adsorption, *International Journal of Nanoelectronics and Materials (IJNeaM),* 17, 101–105.

[22] Bezverkhyy I., Ortiz G., Chaplais G., Marichal C., Weber G., & Bellat JP., 2014, MIL-53 (Al) under reflux in water: Formation of γ-AlO (OH) shell and H2BDC molecules intercalated into the pores, *Microporous and mesoporous materials,* 183, 156-161. https://doi.org/10.1016/j.micromeso.2013.09.015

[23] Tomar S., & Singh VK., 2021, Review on synthesis and application of MIL-53, *Materials Today : Proceedings*, 43, 3291–3296. https://doi.org/10.1016/j.matpr.2021.02.179

[24] Jia Z., Jiang M., & Wu G., 2017, Amino-MIL-53 (Al) sandwich-structure membranes for adsorption of p-nitrophenol from aqueous solutions, *Chemical Engineering Journal,* 307, 283–290. https://doi.org/10.1016/j.cej.2016.08.090

[25] Qin Y., Wang Q., Ge J., & Wu F., 2021, Microwave ultrasound-assisted synthesis of NH2-MIL-53 (Al) for fluorescence detection of organosulfur compounds in model fuel, *Inorganic Chemistry Communications*, 132, 28–33. https://doi.org/10.1016/j.inoche.2021.108828

[26] Yoon S., Park J., Kumar A., Police R., Kwon J., & Bae S., 2025, Enhanced removal of perfluorooctanoic acid by aluminum-based metal – organic frameworks prepared by bauxite residue, *Journal of Hazardous Materials*, *483,* 1-14. https://doi.org/10.1016/j.jhazmat.2024.136687

[27] Zhang Y., Gao Q., Lin Z., Zhang T., Xu J., Tan Y., Tian W., & Jiang L., 2014, Constructing Free Standing Metal Organic Framework MIL-53 Membrane Based on Anodized Aluminum Oxide precursor, *Scientific Reports,* 4(1), 2–7. https://doi.org/10.1038/srep04947

[28] Wang H., Jiang Y., Han R., Liu Q., & Liu C., 2025, Facile preparation of Al/Mn bimetallic metal-organic frameworks for removing trace benzene indoor, *Separation and Purification Technology*, 354, 1-10. https://doi.org/10.1016/j.seppur.2024.128625

[29] Wang X., & Jacobson AJ., 2016, Hydrothermal crystal growth and Vernier structures of the metal benzenedicarboxylates MIL-47 and MIL-53 containing guest molecules of benzenecarboxylic acid, *Journal of Solid State Chemistry*, 236, 230–235. https://doi.org/10.1016/j.jssc.2015.08.014

[30] Loiseau T., Serre C., Huguenard C., Fink G., Taulelle F., Henry M., ... Férey G., 2004, A rationale for the large breathing of the porous aluminum terephthalate (MIL-53) upon hydration, *Chemistry–A European Journal*, 10(6), 1373-1382. https://doi.org/10.1002/chem.200305413

[31] Khodayari A., & Sohrabnezhad S., 2021, Fabrication of MIL-53 (Al)/Ag/AgCl plasmonic nanocomposite : An improved metal organic framework based photocatalyst for degradation of some organic pollutants, *Journal of Solid State Chemistry,* 297, 1-16. https://doi.org/10.1016/j.jssc.2021.122087

[32] Guo Z., Wu N., Wu Y., Sun C., Wu H., & Li Q., 2022, Anion-induced morphology control of Al-fumarate MOFs via synergetic coordination and hydrogen bond effects for graded dehumidification, *Microporous and Mesoporous Materials*, 343, 1-10. https://doi.org/10.1016/j.micromeso.2022.112168